



Realization of a $SU(2) \times SU(6)$ System of Fermions in a Cold Atomic Gas

Shintaro Taie,^{1,*} Yosuke Takasu,¹ Seiji Sugawa,¹ Rekishu Yamazaki,^{1,2} Takuya Tsujimoto,¹
Ryo Murakami,¹ and Yoshiro Takahashi^{1,2}

¹Department of Physics, Graduate School of Science, Kyoto University, Japan 606-8502

²CREST, JST, 4-1-8 Honcho Kawaguchi, Saitama 332-0012, Japan

(Received 19 May 2010; revised manuscript received 12 August 2010; published 1 November 2010)

We report the realization of a novel degenerate Fermi mixture with an $SU(2) \times SU(6)$ symmetry in a cold atomic gas. We successfully cool the mixture of the two fermionic isotopes of ytterbium ^{171}Yb with the nuclear spin $I = 1/2$ and ^{173}Yb with $I = 5/2$ below the Fermi temperature T_F as $0.46T_F$ for ^{171}Yb and $0.54T_F$ for ^{173}Yb . The same scattering lengths for different spin components make this mixture featured with the novel $SU(2) \times SU(6)$ symmetry. The nuclear spin components are separately imaged by exploiting an optical Stern-Gerlach effect. In addition, the mixture is loaded into a 3D optical lattice to implement the $SU(2) \times SU(6)$ Hubbard model. This mixture will open the door to the study of novel quantum phases such as a spinor Bardeen-Cooper-Schrieffer-like fermionic superfluid.

DOI: 10.1103/PhysRevLett.105.190401

PACS numbers: 05.30.Fk, 03.75.Ss, 37.10.Jk, 67.85.Lm

While $SU(2)$ symmetry is ubiquitous in nature, realization of an $SU(N)$ symmetry with $N > 2$ in condensed matter physics is a rather special case. A system with higher symmetry is expected to show novel behaviors in both qualitative and quantitative ways. One remarkable example is the Kondo effect in quantum dots, in which the $SU(4)$ symmetry due to orbital degeneracy considerably increases the Kondo temperature, compared to the $SU(2)$ case [1]. The $SU(4)$ symmetry is also approximately realized in graphene, and relevant quantum Hall magnetism is discussed [2]. Ultracold atomic gases seem to be good candidates for exploring the physics of $SU(N)$ because of their variety of spin degrees of freedom and high controllability. However, it is difficult, though not impossible [3], to realize enlarged spin symmetries with alkali atoms because of their complicated hyperfine structures. This difficulty can be overcome by using fermionic isotopes of alkaline-earth-metal-like atoms in which the absence of electronic spin in the ground states decouples their nuclear spin from collision processes. In this case, the scattering lengths for any combination of spin components are the same, resulting in an $SU(2I + 1)$ symmetry for nuclear spin I [4,5]. Recently, multicomponent fermions with higher symmetry attract much attention and the presence of rich quantum phases are predicted [3–6]. In particular, a system of two-orbit $SU(N)$ symmetry is intensively discussed in Refs. [5,7].

In this Letter, we report the realization of a two-species Fermi-Fermi degenerate gas mixture with a novel $SU(2) \times SU(6)$ spin symmetry. This is attained by applying an all-optical evaporative cooling method to two ytterbium (Yb) fermionic isotopes of ^{171}Yb with the nuclear spin $I = 1/2$ and ^{173}Yb with $I = 5/2$. While the spin-polarized two-species Fermi-Fermi mixture [8] is attractive to study many unexplored quantum phenomena [9], it is natural to expect rich quantum phases with the Fermi-Fermi mixture with

the $SU(2) \times SU(6)$ spin symmetry [5,7]. As a first step, we load the mixture into a 3D optical lattice to implement the $SU(2) \times SU(6)$ Hubbard model where a variety of quantum phases has been recently discussed [5]. Another intriguing example is the possibility of a spinor Bardeen-Cooper-Schrieffer (BCS)-like fermionic superfluidity discussed in Ref. [10] where an interesting similarity between the heteronuclear superfluids and spinor BEC at the mean-field level has been pointed out.

The experimental procedure for preparing a mixture of two Yb isotopes is described in detail in Ref. [11] and we briefly summarize the method. Figure 1 shows the schematic view of our experimental setup. Yb atoms are loaded

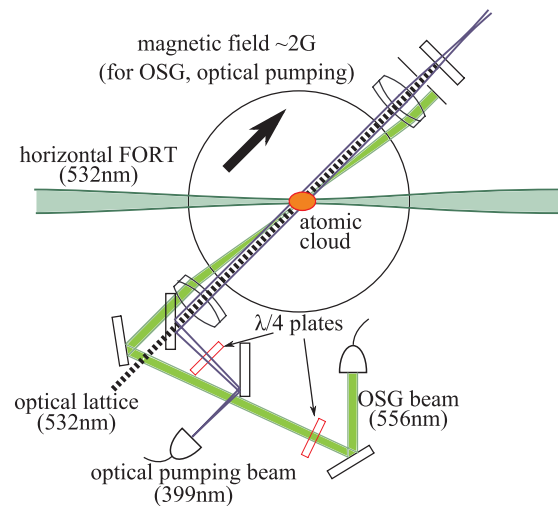


FIG. 1 (color online). Experimental setup. Laser beams for the OSG separation, optical pumping, and an optical lattice are shown. The OSG laser beam, whose wavelength is close to that of the lattice, is slightly tilted with respect to others. This does not cause any serious errors in the observed spin population.

into a magneto-optical trap (MOT) with the $^1S_0 \leftrightarrow ^3P_1$ transition ($\lambda = 556$ nm) after the deceleration by a Zeeman-slower using the $^1S_0 \leftrightarrow ^1P_1$ transition ($\lambda = 399$ nm). Next, the two isotopes are loaded into a crossed far-off-resonant trap (FORT) with 532 nm light. The sympathetic evaporative cooling is performed by continuously decreasing the FORT trap depth. We note that both isotopes are cooled with full spin mixtures, as described later. From our previous photoassociation study [12], the small s -wave scattering length of -0.15 nm is known for ^{171}Yb , whereas that for ^{173}Yb is as large as 10.55 nm. We can employ efficient evaporative cooling of ^{171}Yb with ^{173}Yb through the large interspecies scattering length of -30.6 nm. Theoretical estimate shows that the relative difference of scattering lengths for nuclear spin states of alkaline earth atoms is on the order of 10^{-9} [5]. Experimentally, no visible splitting in the photoassociation resonance for ^{173}Yb was found in Ref. [12], which supports the SU(6) symmetry of ^{173}Yb . The residual magnetic field is estimated to be smaller than 20 mG by measuring the Zeeman splitting of the ultranarrow $^1S_0 \leftrightarrow ^3P_2$ transition. The corresponding nuclear Zeeman energy in the ground state is on the order of 10 Hz for both isotopes.

Before we describe the results for the two-species mixture, we show the results for single-species Fermi gas of ^{173}Yb with an SU(6) symmetry to illustrate the nuclear spin selective imaging with an Optical Stern-Gerlach (OSG) effect. The spin selective imaging or detection is crucially important in many studies of Fermi gases with spin degrees of freedom. The separate imaging of each nuclear spin components is, however, very difficult with a usual Stern-Gerlach effect due to the small nuclear magnetic moments. Here in this work we successfully overcome this difficulty by exploiting the OSG effect produced by an off-resonant circularly polarized laser beam [13]. It is noted that the spin-dependent light shift is the origin of the fictitious magnetic field considered here [14]. Figure 2(a) shows

absorption images of pure ^{173}Yb degenerate gases with 6 components without the OSG separation. Here, the $^1S_0 \leftrightarrow ^1P_1$ transition is used for imaging. The fit to the Thomas-Fermi profile yields the temperature of $0.14T_F$ and the number of atoms of 5.0×10^4 . The Fermi temperature is given by $T_F = (6N/s)^{1/3} \hbar \omega / k_B$, where N is atom number, $s = 6$ for ^{173}Yb is the number of degenerate states, \hbar is the Planck constant divided by 2π , ω is mean trap frequency, and k_B is the Boltzmann constant.

While the achievement of quantum degeneracy of ^{173}Yb has already been reported [15], the spin population was not investigated. Figure 2(b) shows a schematic view of the OSG experiment. The OSG beam is focused just above the atom cloud with the waist of about $100 \mu\text{m}$ to provide the atoms an dipole force due to the potential gradient. In this measurement, the pulse with the duration of 2.5 ms, the beam power of 4 mW, and the detuning of about +1 GHz with respect to the $^1S_0(F_g = 5/2) \leftrightarrow ^3P_1(F_e = 7/2)$ transition of ^{173}Yb is used. Figure 2(c) shows the separately observed images of spin components of ^{173}Yb . Figure 2(d) shows the simulated distributions under the present experimental condition and assumption of no spin polarization. The overall feature of the observed distributions can be reproduced. The distortion of the initially isotropic momentum distribution is caused by the nonuniform intensity gradient of the OSG beam. In order to image ^{173}Yb atoms with $m_F = -5/2$ and $m_F = -3/2$ states separately, we repeat the measurement with an opposite sense of circular polarization for the OSG beam. We find that the relative imbalance of the spin population is smaller than 5%, which shows almost no spin polarizations. The slight imbalance can come from the initial preparation. The demonstrated technique is very useful for investigating the novel magnetism induced for a system with high spin symmetry.

Next we describe the experimental results for two-species Fermi-Fermi mixture. Figure 3 shows absorption images obtained after the final stage of the evaporative

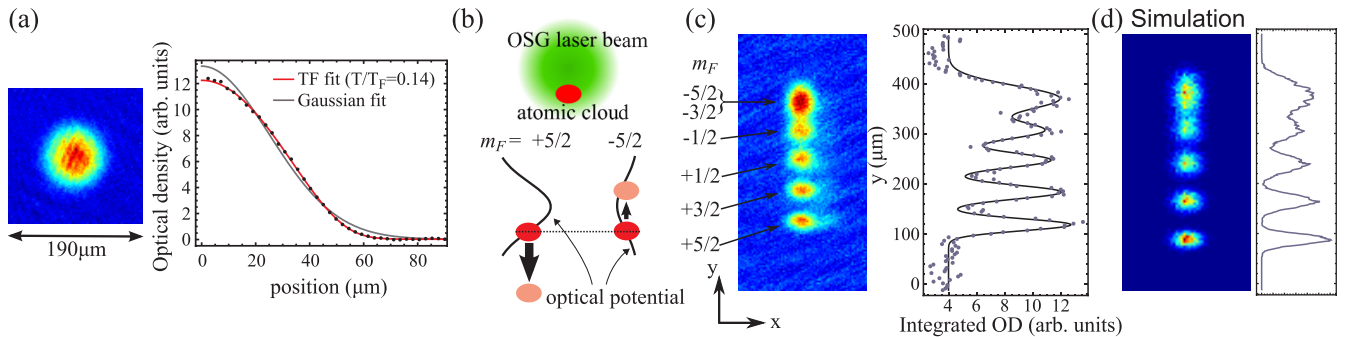


FIG. 2 (color online). Optical Stern-Gerlach separation of nuclear spins. (a) Time-of-flight image of a degenerate Fermi gas of ^{173}Yb without the OSG separation. The image is taken after 12 ms ballistic expansion. The azimuthally averaged distribution is also shown on the right hand side. The temperature of $0.14T_F$ is determined from the Thomas-Fermi fit (red line). The observed distribution clearly deviates from the classical Gaussian shape, indicated by the gray line. (b) Schematic view of an OSG effect. The atoms in the $m_F = +5/2$ state is pushed downward in the figure, whereas the $m_F = -5/2$ upward. (c) Optical Stern-Gerlach separation of spin components in the Fermi gas of ^{173}Yb . The expansion time is 8 ms. Integration of the images along the horizontal axis are also shown on the right hand side. (d) The simulated distribution under the current experimental condition is shown.

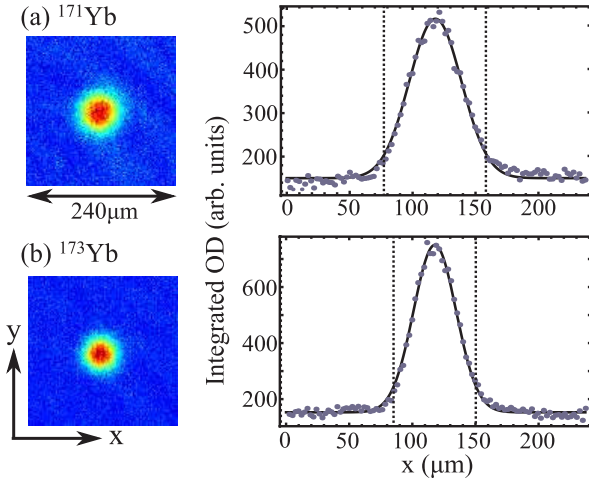


FIG. 3 (color online). Time-of-flight images of the quantum degenerate Fermi-Fermi mixture with spin degrees of freedom, (a) for two-spin mixture of ^{171}Yb and (b) for 6-spin mixture of ^{173}Yb . The expansion time is 9 ms for ^{171}Yb and 8 ms for ^{173}Yb . The density distributions integrated over the vertical direction y are also shown on the right hand side. From the Gaussian fits we can estimate the temperatures $T = 95$ nK and $T = 87$ nK for ^{171}Yb and ^{173}Yb , respectively. The dotted lines correspond to the Fermi velocities $v_F = \sqrt{2k_B T_F/m}$ for each isotope. The images are averaged over 5 independent measurements.

cooling. Starting from the 2×10^5 ^{171}Yb and 8×10^5 ^{173}Yb atoms in the FORT, about 12 s evaporation results in the coldest temperatures of less than 100 nK. It is noted that the image of each isotope is taken using the two independent probe beam with a sequential measurement for the same sample. We fit the measured momentum distribution with a Gaussian distribution and obtain the atom numbers of ^{171}Yb and ^{173}Yb are 8.0×10^3 and 1.1×10^4 , respectively. The temperatures are 95 nK for ^{171}Yb and 87 nK for ^{173}Yb , and we estimate T/T_F to be 0.46 for ^{171}Yb , and 0.54 for ^{173}Yb , respectively [16]. In this temperature regime, the fits with the Fermi-Dirac distribution give almost the same value for T/T_F as the Gaussian distributions. We also note that this is the first realization of a quantum degenerate gas of ^{171}Yb .

The OSG separation is also applied to the mixture gas of ^{171}Yb and ^{173}Yb . The same detuning of OSG laser light as used for pure ^{173}Yb sample is also applicable for simultaneously separate the nuclear spin components of both isotopes. Again, we confirm that the atoms are almost equally distributed over all nuclear spin states for both ^{171}Yb and ^{173}Yb [see Figs. 4(a) and 4(b)].

It is worth noting that by applying optical pumping to ^{173}Yb via the $^1S_0(F_g = 5/2) \leftrightarrow ^3P_1(F_e = 3/2)$ transition, we can prepare an almost equal mixture of $m_F = +3/2$ and $m_F = +5/2$ states. By numerically simulating the rate equations, we find that the relative imbalance is on the order of 10^{-4} , assuming perfect light polarization and balanced initial spin population. In this case, conservation

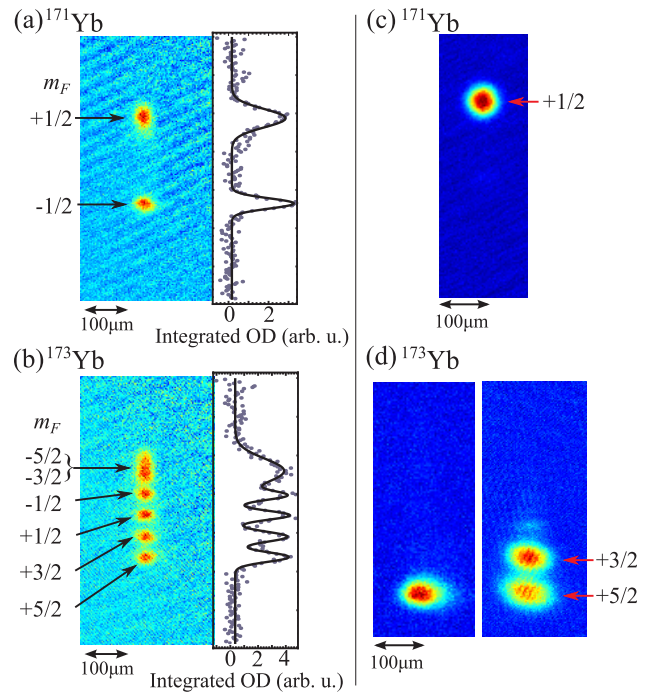


FIG. 4 (color online). Left: Optical Stern-Gerlach separation of spin components in the $^{171}\text{Yb} - ^{173}\text{Yb}$ quantum degenerate mixture (a) for ^{171}Yb and (b) for ^{173}Yb . The expansion time is 6 ms and the images are averaged over 8 independent measurements. Integrations of the images along the horizontal axis are also shown on the right hand side. Right: Spin manipulation by optical pumping, applied to single-species samples. (c) The OSG separation is applied after optical pumping to the $m_F = +1/2$ state of ^{171}Yb . (d) For ^{173}Yb , optical pumping allows us to prepare either a single-component gas in the $m_F = +5/2$ state (left) or a two-component mixture of the $m_F = +3/2$ state and the $m_F = +5/2$ state (right).

of the atom numbers with each spin leads to an reduced $\text{SU}(2) \times \text{SU}(2)$ symmetry [5]. In addition, optical pumping also enables to create a spin-polarized mixture of ^{171}Yb and ^{173}Yb . Here, the $^1S_0 \leftrightarrow ^1P_1$ ($F_e = F_g$) transition is used for optical pumping. The polarized mixture is cooled down via interspecies collisions only, and the suppression of three-body losses allows us to cool the sample down to lower temperature, $0.33T_F$ for ^{171}Yb and $0.30T_F$ for ^{173}Yb . The spin distribution after optical pumping is examined by the OSG separation and shown in Figs. 4(c) and 4(d).

Finally, the mixture is successfully loaded into a 3D optical lattice to implement the $\text{SU}(2) \times \text{SU}(6)$ Hubbard model. A variety of quantum phases in such a system is discussed [5]. The 3D lattice is formed with three orthogonal standing waves with a lattice constant d of 266 nm. The quasimomentum distribution spreads over the entire first Brillouin zone as the characteristic density $\rho = Nd^3(m\omega^2/2J)^{3/2}$ [17] increases. Here, m is the atomic mass and J is the hopping matrix element. Figure 5 shows the quasimomentum distribution (a) for ^{171}Yb and (b) for

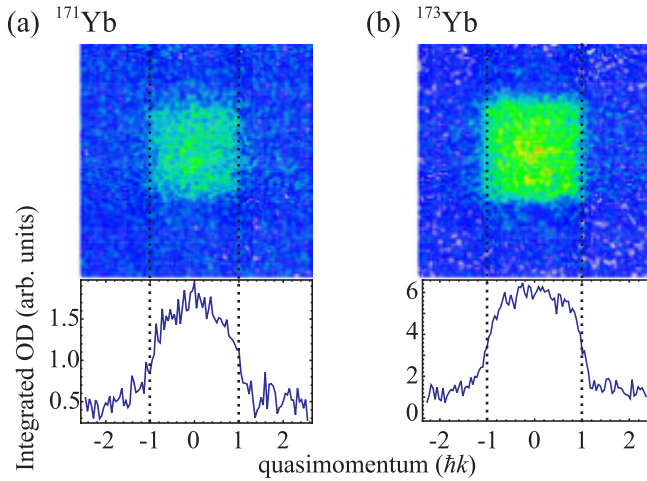


FIG. 5 (color online). Quasimomentum distribution of (a) ^{171}Yb and (b) ^{173}Yb in the $\text{SU}(2) \times \text{SU}(6)$ two-species mixture in an optical lattice. The density distributions integrated along the vertical direction are also shown below. The atom numbers are 0.4×10^4 for ^{171}Yb and 1.5×10^4 for ^{173}Yb , respectively. The images are taken after linear ramping down of the lattice in 0.5 ms, followed by a ballistic expansion of (a) 12 and (b) 13 ms. The dotted lines indicate the domain of the 1st Brillouin zone, which equals twice the recoil momentum $\hbar k$. The tails in the measured distribution may be due to the breakdown of adiabaticity during the band-mapping sequence.

^{173}Yb for the lattice height of $10E_r$, measured by a band-mapping technique. Here E_r is the recoil energy and is about 200 nK in this experiment. The measured distribution indicates an insulating state, which is consistent with the values of ρ calculated as 800 for ^{171}Yb and 3000 for ^{173}Yb [18]. The strong interaction effect is revealed by our recent observation of Bloch oscillations in a 3D optical lattice, which is beyond the scope of this Letter and will be discussed elsewhere.

In conclusion, we demonstrate the successful realization of two-species Fermi-Fermi degenerate gas mixture of the fermionic isotopes of ^{171}Yb with $I = 1/2$ and ^{173}Yb with $I = 5/2$ with spin degrees of freedom. The nuclear spin components for each fermion are separately imaged by exploiting an optical Stern-Gerlach effect. The mixture is successfully loaded into a 3D optical lattice to implement the $\text{SU}(2) \times \text{SU}(6)$ Hubbard model. Exploring spinor BCS-like superfluid or Kondo physics [19] would be the next step. The required temperature seems to be accessible with slight improvement of the current conditions. We expect an efficient optical Feshbach resonance effect to achieve fermionic superfluid due to the large negative interspecies scattering length of -30.6 nm [20,21].

We acknowledge M. A. Cazalilla for first pointing out the $\text{SU}(6)$ symmetry for ^{173}Yb and importance of separate spin detection, and S. Uetake and T. Fukuhara for their experimental help. This work was supported by the Grant-

in-Aid for Scientific Research of JSPS (No. 18204035, 21102005C01 (Quantum Cybernetics), 21104513A03 (DYCE), 22684022), GCOE Program “The Next Generation of Physics, Spun from Universality and Emergence” from MEXT of Japan, FIRST, and Matsuo Foundation. S. T. and S. S. acknowledge supports from JSPS.

*taie@scphys.kyoto-u.ac.jp

- [1] S. Sasaki *et al.*, *Phys. Rev. Lett.* **93**, 017205 (2004).
- [2] K. Nomura and A. H. MacDonald, *Phys. Rev. Lett.* **96**, 256602 (2006).
- [3] C. Honerkamp and W. Hofstetter, *Phys. Rev. Lett.* **92**, 170403 (2004).
- [4] M. A. Cazalilla, A. F. Ho, and M. Ueda, *New J. Phys.* **11**, 103033 (2009).
- [5] A. V. Gorshkov *et al.*, *Nature Phys.* **6**, 289 (2010).
- [6] C. Wu, J. P. Hu, and S. C. Zhang, *Phys. Rev. Lett.* **91**, 186402 (2003); C. Wu, *Mod. Phys. Lett. B* **20**, 1707 (2006); M. Hermele, V. Gurarie, and A. M. Rey, *Phys. Rev. Lett.* **103**, 135301 (2009).
- [7] C. Xu, *Phys. Rev. B* **81**, 144431 (2010).
- [8] M. Tagliaberi *et al.*, *Phys. Rev. Lett.* **100**, 010401 (2008).
- [9] W. V. Liu and F. Wilczek, *Phys. Rev. Lett.* **90**, 047002 (2003); T. Mizushima, K. Machida, and M. Ichioka, *Phys. Rev. Lett.* **94**, 060404 (2005); D. E. Sheehy and L. Radzihovsky, *Phys. Rev. Lett.* **96**, 060401 (2006); M. Iskin and C. A. R. Sá de Melo, *Phys. Rev. Lett.* **99**, 080403 (2007).
- [10] D. B. M. Dickerscheid, Y. Kawaguchi, and M. Ueda, *Phys. Rev. A* **77**, 053605 (2008).
- [11] T. Fukuhara *et al.*, *Phys. Rev. A* **79**, 021601(R) (2009).
- [12] M. Kitagawa *et al.*, *Phys. Rev. A* **77**, 012719 (2008).
- [13] T. Sleator *et al.*, *Phys. Rev. Lett.* **68**, 1996 (1992).
- [14] C. Cohen-Tannoudji and J. Dupont-Roc, *Phys. Rev. A* **5**, 968 (1972).
- [15] T. Fukuhara *et al.*, *Phys. Rev. Lett.* **98**, 030401 (2007).
- [16] The strong attractive interaction between ^{171}Yb and ^{173}Yb can affect the width of the measured momentum distribution. We estimate the increase in the trap frequency due to the mean-field potential to be 20%–30%, resulting in the reduction of the actual T/T_F . On the contrary, the conversion of the negative interaction energy into the kinetic energy during the expansion time causes the underestimation of the temperature by $\sim 10\%$. Therefore we can expect that the actual T/T_F of the sample is $\sim 15\%$ lower than that reported in the text.
- [17] M. Rigol and A. Muramatsu, *Phys. Rev. A* **69**, 053612 (2004).
- [18] M. Köhl *et al.*, *Phys. Rev. Lett.* **94**, 080403 (2005).
- [19] M. Foss-Feig, M. Hermele, and A. M. Rey, *Phys. Rev. A* **81**, 051603(R) (2010).
- [20] K. Enomoto *et al.*, *Phys. Rev. Lett.* **101**, 203201 (2008).
- [21] R. Ciuryło, E. Tiesinga, and P. S. Julienne, *Phys. Rev. A* **71**, 030701(R) (2005).